Weierstraß-Institut
für Angewandte Analysis und Stochastik

Leibniz-Institut im Forschungsverbund Berlin e. V.

Preprint ISSN 2198-5855

Numerical study of coherence of optical feedback in semiconductor laser dynamics

Mindaugas Radziunas[1,2], Douglas J. Little[2], Deborah M. Kane[2]

submitted: July 2, 2019

[1] Weierstrass Institute
Mohrenstr. 39
10117 Berlin
Germany
E-Mail: mindaugas.radziunas@wias-berlin.de

[2] MQ Photonics Research Centre and
Dept. of Physics and Astronomy
Macquarie University
Sydney, NSW 2109
Australia
E-Mail: douglas.little@mq.edu.au
deb.kane@mq.edu.au

No. 2604
Berlin 2019

2010 *Mathematics Subject Classification.* 78A60, 37N20, 35Q60, 78-04, 60G15.

2010 *Physics and Astronomy Classification Scheme.* 42.55.Px, 42.60.Mi, 42.65.Sf, 42.25.Kb, 42.60.Da.

Key words and phrases. Semiconductor lasers, modeling, dynamics, optical feedback, coherence, external cavity, traveling wave.

This work was partially funded by the Macquarie University Faculty of Science and Engineering Visiting Researcher Fellowship awarded to MR.

Edited by
Weierstraß-Institut für Angewandte Analysis und Stochastik (WIAS)
Leibniz-Institut im Forschungsverbund Berlin e. V.
Mohrenstraße 39
10117 Berlin
Germany

Fax: +49 30 20372-303
E-Mail: preprint@wias-berlin.de
World Wide Web: http://www.wias-berlin.de/

Numerical study of coherence of optical feedback in semiconductor laser dynamics

Mindaugas Radziunas, Douglas J. Little, Deborah M. Kane

Abstract

The nonlinear dynamics of semiconductor laser with coherent, as compared to incoherent, delayed optical feedback systems have been discussed and contrasted in prior research literature. Here, we report simulations of how the dynamics change as the coherence of the optical feedback is systematically varied from being coherent to incoherent. An increasing rate of phase disturbance is used to vary the coherence. An edge emitting, 830 nm, Fabry Perot semiconductor laser with a long external cavity is simulated. Following this study, consideration of prior and future experimental studies should include evaluation of where on the continuum of partial coherence the delayed optical feedback sits. Partial coherence is a parameter that will affect the dynamics.

Semiconductor laser with delayed optical feedback (SLDOF) systems have been a topic of sustained research interest for several decades. This is by virtue of their nonlinear dynamics that can be both theoretically modeled and experimentally studied, making these excellent systems for connecting theoretical understanding and experiment in nonlinear science. Also their relevance and uptake in technological applications has been strong [1, 2, 3]. SLDOFs, and integrated device analogs, are researched for applications such as random number generation [2] and information processing using delay photonic systems [4, 5]. Using synchronization in master/slave configurations, they also have applications in secure communications [1, 2, 3] and key generation and exchange [6].

A typical SLDOF system uses a commercially available semiconductor laser, usually, with a high reflectance coating on one end facet of the chip ($> 95\%$) and a low reflectance coating ($< 5\%$) on the other. The main output power emission from the low reflectance facet is collimated and propagates to an external plane mirror. A fraction of the reflected light is coupled back into the semiconductor laser (SL). The main experimental variables used to study systematic changes in the dynamic state of the output power are the strength of the delayed optical feedback, the injection current to the semiconductor laser, and the time τ the light propagates in free space before being coupled back into the SL. Even though the time τ is not easily changed in experimental systems, it was a key variable in the seminal work which first drew attention to the regimes of nonlinear dynamics in the SLDOF system [7]. In particular the sharp transition to coherence collapse [8] was noted. A more recent work [9] has given an update on the original, now-famous plot of regimes of operation (I-V, regime IV being coherence collapse) as a function of cavity length and feedback strength [7]. The assumption that is made in most theoretical models of SLDOF systems [1, 2, 3], either explicitly or implicitly, is that the optical feedback field is coherent. Among the extensive range of different types of delayed optical feedback that have been researched, incoherent feedback has been among them. There is some ambiguity in the literature about what is meant by coherent versus incoherent feedback. Historically, there has been an understanding, not always made explicit, that shorter external cavities (ECs) will have coherent feedback. The large linewidths of order $100 - 200$ MHz for free running Fabry-Perot (FP)-type SLs surprised when first observed [10]. Such linewidths mean an EC with round trip length of order $1 - 2$ meters would have an optical feedback field that was at best partially coherent on temporal coherence

DOI 10.20347/WIAS.PREPRINT.2604 Berlin 2019

grounds. Long EC systems have been reported as having incoherent feedback on this basis [11]. It is also the case that the optical feedback field is not an ideal plane wave after it has been propagated through the collimating and refocusing lens. Differences in the wavefront shape of the feedback field as compared to the emitted field have been visualized through interference fringes and changes in beam profile due to destructive interference [12, 13]. Such variations in spatial coherence can be thought of as effective phase shifts in the one-dimensional propagation model.

A systematic approach to achieving incoherent feedback in experimentally studied semiconductor laser systems has been to rotate the polarization of the feedback field by 90° so that the emitted TE mode is fed back into the TM mode. There are many cases of this approach in the literature, especially applied to vertical cavity surface emitting lasers where polarization dynamics are prevalent. Application to FP SLs has shown that delayed incoherent feedback leads to differentiable non-linear dynamics as compared to coherent feedback, with a major feature being the suppression of the reduced threshold current as the optical feedback fraction increases at a given injection current [14, 15]. Theory for the system has been implemented with a modified Lang-Kobayashi model valid for weak feedback levels [14], and a modified traveling wave model [15]. The incoherent nature of the optical feedback is treated by including it in the dynamics for the carrier density only, and omitting it from the coupled photon density rate equation (L-K model, [14]) or the slowly varying complex field traveling wave equations [15]. In [14] experiments were completed which aimed to investigate a mixture of coherent and incoherent delayed optical feedback by using a quarter wave plate to rotate the polarization of the optical feedback field by 45°. From these results the authors concluded that dynamics with a mixture of coherent and incoherent feedback is most likely the dynamics that are reported from experimental systems. This means that experiments carried out in different labs using the same device in similar but not identical systems may embody differences in the partial coherence state of the delayed optical feedback and, in turn, differences in the observed dynamics. Such differences have been observed and continue to be a topic of informal discussion. Theoretical study of the change in dynamics due to systematically changing the coherence of the feedback is the main topic of this letter.

For simulations of the spatiotemporal dynamics in the FP-type diode laser a traveling wave (TW) model is used. It is a 1(space)+1(time) dimensional system of partial differential equations describing the longitudinal and temporal evolution of complex slowly-varying counter-propagating optical fields, $E^+(z,t)$ and $E^-(z,t)$, complex polarization functions $P^+(z,t)$ and $P^-(z,t)$, and the carrier density $N(z,t)$ [16]:

$$
\begin{aligned}
&\frac{n_g}{c_0}\partial_t E^\pm \pm \partial_z E^\pm = \big[-i\beta(N,|E|^2) - \mathcal{D}\big]E^\pm + F^\pm_{\rm sp},\\
&\beta = \delta_0 + \frac{\alpha_H g'(N-N_{\rm tr})}{2} + i\frac{g_{\rm tot}-\alpha_0}{2}, \qquad g_{\rm tot} = \frac{g'(N-N_{\rm tr})}{1+\varepsilon|E|^2},\\
&\mathcal{D}E^\pm = \frac{\bar g}{2}(E^\pm - P^\pm), \qquad \frac{\lambda_0^2}{2\pi c_0}\partial_t P^\pm = \frac{\bar\gamma}{2}(E^\pm - P^\pm) - i\bar\lambda P^\pm,\\
&\partial_t N = J(z,t) - \frac{N}{\tau_N} - \frac{c_0}{n_g}\Re\sum\nolimits_{\nu=\pm}\bar E^\nu(g_{\rm tot}-2\mathcal{D})E^\nu,\\
&J(z,t) = \frac{1}{qLwd}\Big(I - \frac{U_F'}{R_s}\Big[N(z,t) - \frac{1}{L}\int_{-L}^{0} N(z',t)dz'\Big]\Big).
\end{aligned}
$$

Here, $|E|^2 = |E^+|^2 + |E^-|^2$ is the local photon density, $\bar E$ denotes the complex conjugate, β, $g_{\rm tot}$, and $F^\pm_{\rm sp}$ are the complex propagation factor, the total gain, and the Langevin noise source contributions to the optical fields. The linear operator $\mathcal{D}$ provides a Lorentzian-shaped approximation of the material gain dispersion with $\bar g$, $\bar\gamma$, and $\bar\lambda$ defining the amplitude, the full width at the half maximum, and the

detuning of the Lorentzian peak from the central reference wavelength λ_0, respectively. $J(z,t)$ models the inhomogeneous injection current.

In our simulations, we have used $\lambda_0 = 830\,\text{nm}$, $\bar{g} = 10^4\,\text{m}^{-1}$, $\bar{\gamma} = 60\,\text{nm}$, $\bar{\lambda} = 0$. Other parameters were the group velocity factor $n_g = 3.7$, the differential gain (including the transverse confinement factor) $g' = 1.036 \cdot 10^{-20}\,\text{m}^2$, the transparency carrier density $N_{\text{tr}} = 10^{24}\,\text{m}^{-3}$, the linewidth enhancement factor $\alpha_H = -3.5$, the internal absorption $\alpha_0 = 6000\,\text{m}^{-3}$, the static frequency (wavelength) detuning $\delta_0 = 0$, the nonlinear gain compression $\varepsilon = 3 \cdot 10^{-23}\,\text{m}^3$, the length of the laser $L = 300\,\mu\text{m}$, the width and depth of the active zone $w = 5\,\mu\text{m}$ and $d = 0.1\,\mu\text{m}$, the carrier lifetime $\tau_N = 2\,\text{ns}$, the derivative of the Fermi level separation $U_F' = 3.5 \cdot 10^{-26}\,\text{V m}^3$, the series resistivity $R_s = 1\,\Omega$, and the injected current I in the range of 0 to $90\,\text{mA}$. c_0 and q are the speed of light in vacuum and the electron charge, respectively. Most of the parameters used in our study have been translated from those used in [13] intended to model an APL-830-40 laser as used in the experimental studies described in [17] and many other published studies. For a detailed explanation of the functions and parameters see also Refs. [16, 18].

At the rear and front facets of the diode, $z = -L$ and $z = 0$, see Fig. 1(a), the optical fields satisfy the reflecting boundary conditions

$$E^+(-L,t) = -\bar{r}_{-L}E^-(-L,t) \qquad \text{and} \qquad E^-(0,t) = r_0E^+(0,t) + t_0F_i(t),$$

where r_{-L} and r_0 are the complex field amplitude reflection coefficients at both facets, the factor $t_0 = \left(1 - |r_0|^2\right)^{1/2}$ defines the field transmission through the front facet, and $F_i(t)$ represents the optical feedback from the conventional EC, when present. The emitted field at the front facet is defined by $F_e(t) = t_0E^+(0,t) - \bar{r}_0F_i(t)$. Here we account for the (usually small) reflection of the incident field from the outer side of the front facet. The EC-induced relation between the emitted and incident beams is

$$E_i(t) = e^{i\zeta(t)}\left[\eta e^{i\varphi}E_e(t-\tau)\right],$$

where η, φ, and τ are the part of emitted field amplitude which returns to the laser diode, the fixed phase change of the complex field amplitude during the field propagation in the EC, and the EC roundtrip time, respectively. The random phase noise factor $\zeta(t)$ is a subject of our study in this work and is neglected when assuming strictly coherent feedback.

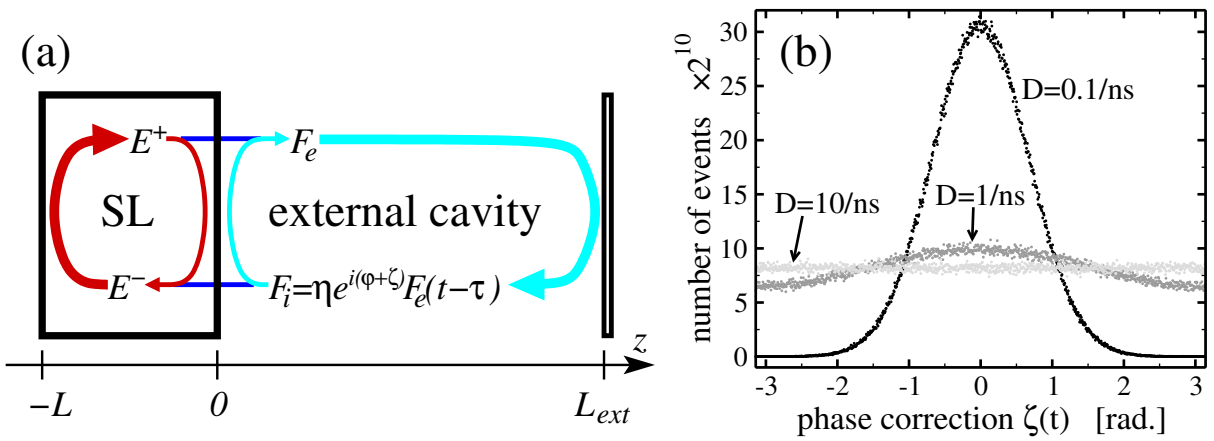

Figure 1: Schematic of a SLDOF system (a) and three histograms (1000 steps over the full phase range) representing random processes $\zeta(t)$ with different variances D used in simulations of $\sim 500\,\text{ns}$ transients (b).

The TW model allows moderate and strong optical feedback regimes to be considered and has been applied successfully to EC diode lasers where the optical length of the EC is comparable to the diode length [11] and also to semiconductor ring lasers [12]. Here-in it is applied to a FP edge emitting semiconductor laser with the rear facet coated for high reflectance, $r_{-L} = \sqrt{0.95}$, and the front facet facing the EC coated for low reflectance, $r_{-L} = \sqrt{0.05}$. In our simulations, we considered the EC defined by $\tau = 4.5$ ns, $\varphi = 0$, and $\eta \leq 0.25$, where $\eta \sim 0.2$ is about the highest feedback achievable in experimental systems using conventional feedback when mode matching, coupling efficiency, and other technical limitations are taken into account. The coherence of the delayed optical feedback field is reduced systematically by introducing several levels of phase noise to the reinjected field at the laser facet facing the EC. The function $\zeta(t)$ represents a Gaussian random process with zero mean. We assume that during propagation within the EC, the field is losing its coherence with the rate D, which defines the variance of the process. For the considered τ, and D not significantly exceeding $0.1/$ns, the phase noise remains concentrated within a limited phase interval centered at 0 (see the black trace in Fig. 1(b)). In this case, we still have some partial coherence of the optical feedback. With the increase of D, the wings of the corresponding distribution spread through the borders of the whole phase interval $[-\pi, \pi]$, and, due to the phase periodicity, reenter the same interval from the opposite side. For $D = 1/$ns some small partial coherence of the feedback is still present, but for $D = 10/$ns it should be lost (see dark and light grey traces in the same figure).

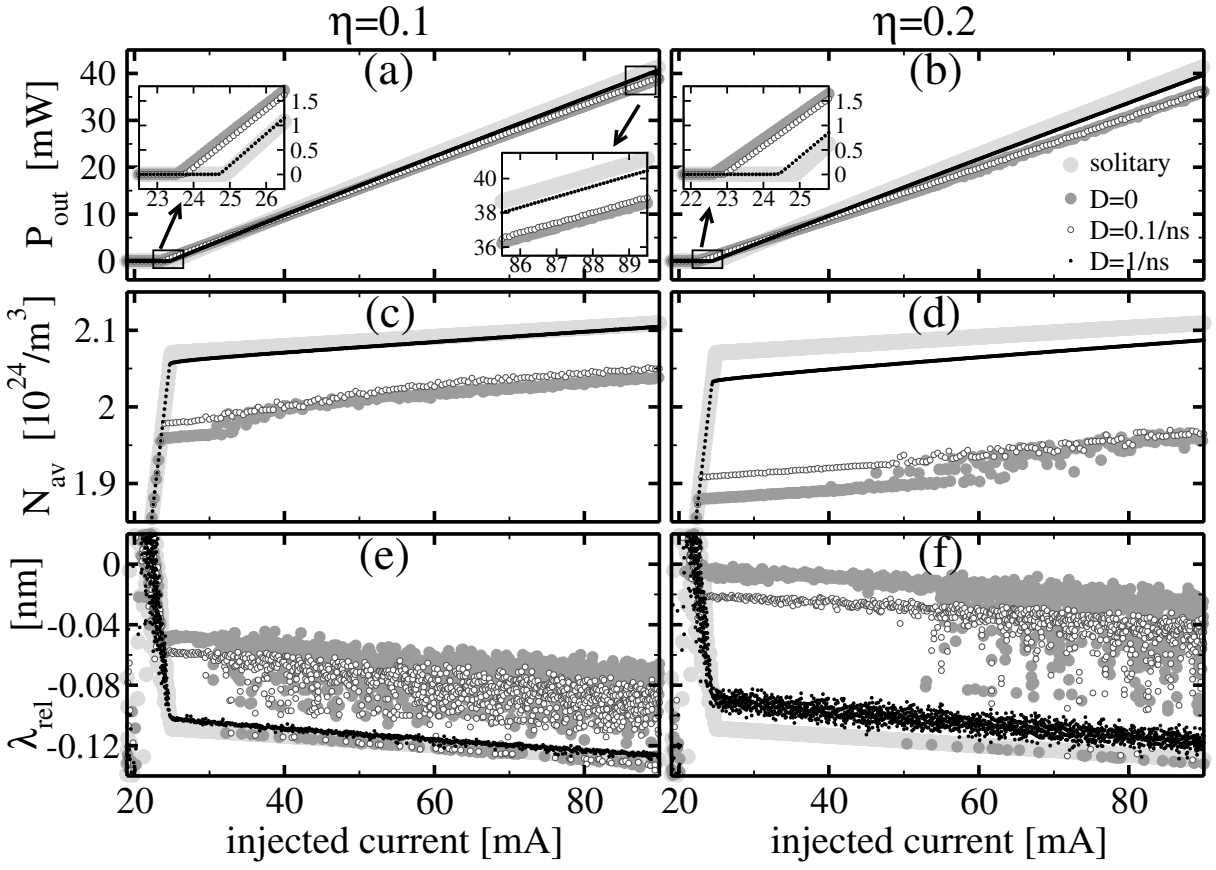

Figure 2: Power of the emitted field at the front facet (a,b), time- and space-averaged carrier densities (c,d), and relative wavelengths of less than by 5 dB distinguishable major peaks of the optical spectra in the vicinity of the central wavelength (e,f) as functions of the injected current for $\eta = 0.1$ (left column) and $\eta = 0.2$ (right column). Thick light gray: solitary laser. Dark gray, empty bullets, and black dots: SLDOFs with the variance D of the phase noise set to 0, $0.1\,\text{ns}^{-1}$, and $1\,\text{ns}^{-1}$, respectively.

To study the impact of the phase noise $\zeta(t)$, we have numerically investigated the performance of the solitary SL and the SLDOF characterized by different η and D with up-sweep of the bias current. The dynamics of the corresponding SL device at each fixed current was estimated from ~ 500 ns post transients (2^{23} time steps in our simulations). The results of these simulations for $\eta = 0.1$ and $\eta = 0.2$ are summarized in the left and right panels of Fig. 2. Thick light gray in all diagrams represents the operation of the solitary SL. Since the gain compression ε is non-vanishing, the total gain $g_{\rm tot}$ of the system is kept at the same level by a slight increase of the (time and space-averaged) carrier density $N_{\rm av}$ (2nd row). Consequently, we also get a linewidth enhancement factor-induced blue shift of the lasing wavelengths $\lambda_{\rm rel}$ (3rd row, shown in the neighborhood of a single resonance of the FP SL).

Let us switch to the discussion of the coherent ($D = 0$) and partially-coherent ($D = 0.1/$ns) feedback in Fig. 2. The expected reduction in the lasing threshold current caused by the feedback is seen in these cases (left inserts in panels (a) and (b)). The reduction is larger when the feedback is larger. A significant reduction of $N_{\rm av}$ and increase of dominant wavelength $\lambda_{\rm rel}$ at each fixed bias in these cases (see 2nd and 3rd line panels of Fig. 2) are implied by the position of the compound cavity mode (CCM) [18, 19] with lowest threshold in the SLDOF system. This lowest threshold mode (LTM) is an analog of the maximal gain external cavity mode in the Lang-Kobayashi model. Multiple spectral peaks in the 3rd-row panels indicate the involvement of several CCMs in the irregular dynamics of the analyzed SLDOF systems.

In the case of entirely incoherent feedback ($D = 1/$ns), the situation is quite different. Since the feedback phase is arbitrary, it is not possible to distinguish the dominant wavelength(s) of the reinjected signal, and the compound cavity modes cannot be defined any more. Instead of providing selection and enhancement of low-threshold CCMs at specific wavelengths, âĂIJnoisyâĂİ optical feedback only excites multiple modes of the solitary FP laser at the wavelengths $\lambda_{\rm FP}$. Incoherent optical feedback implies a small reduction of the total (internal and radiation) losses and, therefore, of the threshold gain in the FP laser. Consequently, the values of $N_{\rm av}$ (or dominant $\lambda_{\rm rel}$) are slightly lower (or higher) than those of the solitary laser, and this difference grows with growing feedback factor η as seen by comparing the thick light gray and small black dots in panels (c), (e) and (d), (f) of Fig. 2. The threshold reduction in this case is nearly absent as seen by comparing the thick light gray and thin black lines in the left inserts of panels (a) and (b). This is consistent with other studies of incoherent optical feedback [14, 15].

Fig. 3 represents typical temporal and spectral behavior of the simulated SLDOF system for different levels of incoherence. When the feedback is coherent ($D = 0$), the dynamics is determined by the interaction of several low-threshold CCMs located in the vicinity of 5-7 modes of the solitary FP laser (see gray peak positions in panel (c)). Optical feedback mimics the emitted field (see black dots in the same panel). The resulting irregularly oscillating time trace of the emission (panel (a)) has several periods. Two smaller of these, namely the period corresponding to the relaxation-oscillation frequency $f_{\rm RO}$ within 5-10 GHz range and the period determined by the spectral separation of the solitary FP modes, $f_{\rm FP} = c_0/2Ln_g \approx 135$ GHz, are hardly visible in the time-domain representation (panel (a)) but are well represented by the radiofrequency (RF) spectra of the calculated emission (panel (b)). Much larger periods of low-frequency fluctuations ($f_{\rm LFF} \approx 14$ MHz) or EC roundtrip ($f_{\rm EC} = 1/\tau \approx 222$ MHz) can be recognized when inspecting the time-trace or the RF spectrum in the small frequency region (inset in panel (b)). It is noteworthy that RF frequency components in $40 - 100$ GHz range, as well as optical frequencies between the FP laser resonances (panel (c)), are well suppressed. An increase of factor D up to $D = 0.1/$ns, see Fig. 3(d-f), preserves the main features of the dynamics. The difference from the strictly coherent case is a growth of both the previously suppressed frequencies in the RF spectra (panel (e)) and the background noise floor in the optical feedback and emission spectra (panel (f)). Moreover, a partially incoherent feedback excites further CCMs in the vicinity of more distant FP

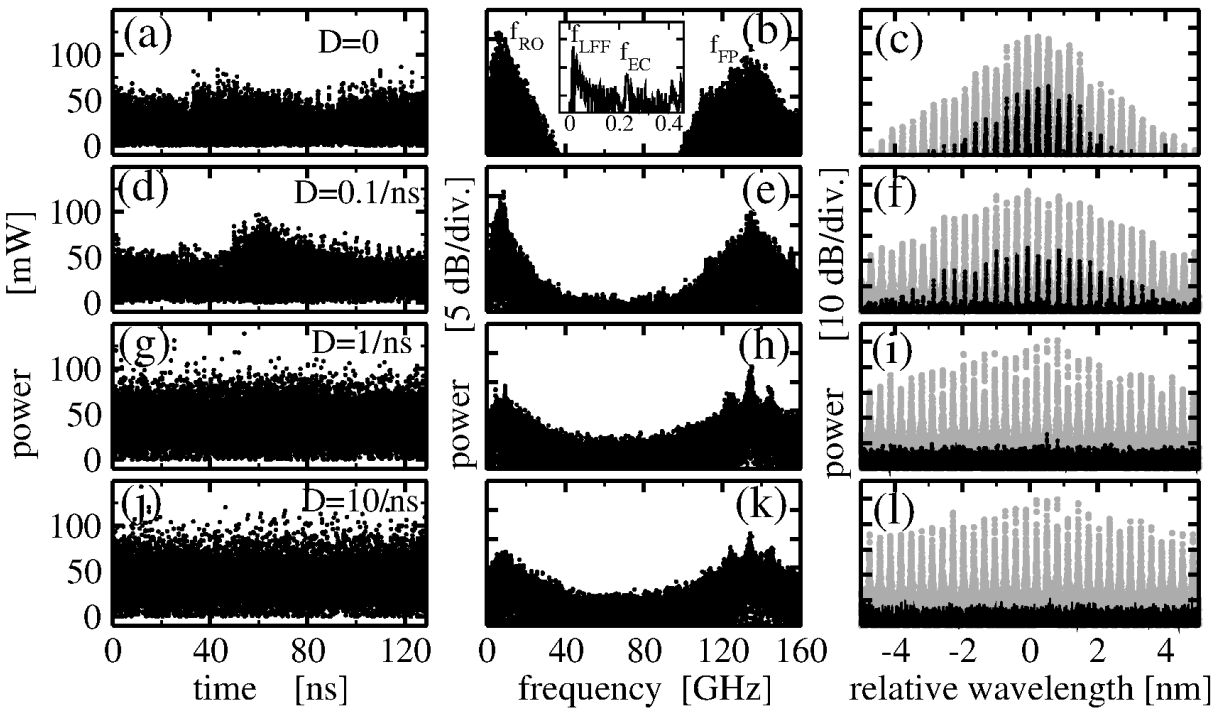

Figure 3: Simulated emitted field intensity time traces (left panels), their radiofrequency spectra (middle panels), optical spectra of the emitted and reinjected fields (gray and black in the right panel figures) for incoherence rate D set to 0 (a-c), $0.1\,\mathrm{ns}^{-1}$ (d-f), $1\,\mathrm{ns}^{-1}$ (g-i), and $10\,\mathrm{ns}^{-1}$ (j-l). In all cases, $\eta = 0.1$ and $I = 55\,\mathrm{mA}$.

resonances (compare widths of the spectral envelopes in panels (c) and (f)). A further reduction of coherence using $D = 1/\mathrm{ns}$ (panels (g-i)) and $D = 10/\mathrm{ns}$ (j-l) implies a total flattening of the optical spectrum of reinjection (black dots in panels (i) and (l)) and, therefore, a growth of the background noise floor in the optical spectra of emission and a further flattening of the RF spectrum (panels (h) and (k)). The presence of the small frequencies f_{LFF} and f_{EC} is not visible in the time-traces nor in the low-frequency range of the RF spectra. The remnants of coherence in the case $D = 1/\mathrm{ns}$ are represented by two small spectral peaks of the optical feedback at $\lambda_{\mathrm{rel}} \in [0.5, 1]$ nm (see black spectra in panel (i)), which is consistent with a still recognizable mean value of $\zeta(t)$ (dark gray histogram in Fig. 1(b)).

A systematic numerical study of the transition from the coherent to fully-incoherent feedback is represented in Fig. 4. Here, we show the predominantly chaotic dynamics of the SLDOF system with growing optical feedback (abscissa axis of each diagram) for different values of D (different panels, with the coherent feedback case $D = 0$ at the left and entirely incoherent case $D = 10/\mathrm{ns}$ at the right). In the top images, for rates of $D \leq 0.2/\mathrm{ns}$, the dominant λ_{rel} increases with optical feedback, as is expected for coherent feedback. The optical bandwidth broadens: it tends to, at best, cover the wavelength range between the feedback-governed higher wavelength λ_{LTM} of the least threshold CCM and the lower wavelength λ_{FP} of the solitary laser resonance. There is an increasing trend to a narrower optical bandwidth about λ_{LTM} as the optical feedback factor, η, increases. The inspection of the RF spectra (lower diagrams in Fig. 4) for $\eta \lesssim 0.15$ reveals the persistence of several typical frequencies, which are f_{LFF} (intensive colors at low frequencies), f_{EC} (characterizing separation of periodically reappearing spectral peaks represented by multiple horizontal intensive-color stripes), relaxation oscillation frequency f_{RO} ($\sim 5\,\mathrm{GHz}$ for the solitary laser), and another feedback-induced frequency f_{FI} growing with η up to 15 GHz. This growth of f_{FI} correlates with the simultaneously

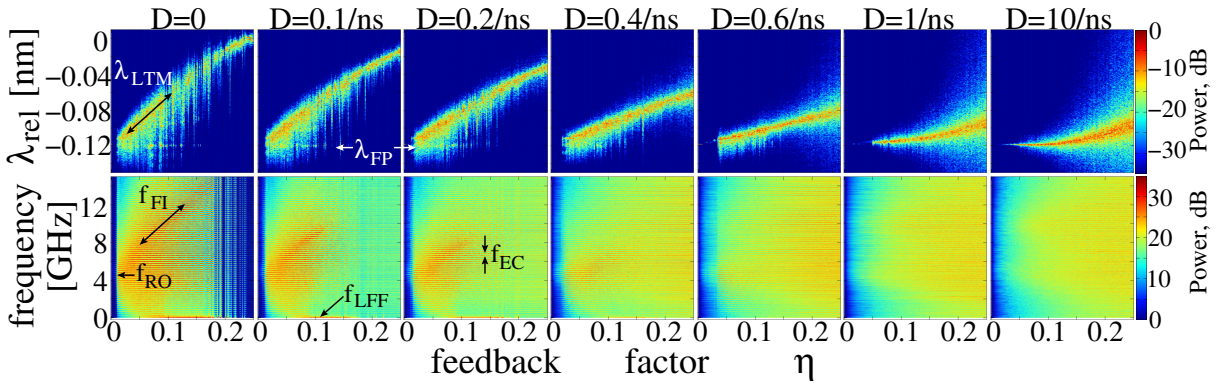

Figure 4: Mappings of simulated optical spectra in the vicinity of a central solitary FP laser resonance (top) and RF spectra for small-to-moderate frequencies (bottom) for different incoherence factors D (indicated at the top of upper diagrams) as functions of optical feedback level η. In all cases, $I = 55$ mA.

increasing separation of λ_{LTM} and λ_{FP} (cf. corresponding upper diagrams).

With increasing D, the initially concave red-shift of the central lasing mode gradually decreases and flattens (upper diagrams for $D < 1/\mathrm{ns}$), whereas the RF spectrum becomes flatter and loses the majority of previously visible spectral peaks for the broad range of η (corresponding lower diagrams). Once D reaches $1/\mathrm{ns}$ or is larger, the phase of the reinjected field is entirely random and the dominant wavelength remains at λ_{FP}, with just a small convex increase for the higher feedback value (see two upper-right panels of Fig. 4). The RF spectra remain flat (see also Fig. 3(k)) for all feedback values implying irregular dynamics of the SLDOF system.

The form of the broadening of the optical spectrum in the vicinity of a given λ_{FP} is informative. For partially coherent feedback (Fig. 4, $D \leq 0.2/\mathrm{ns}$), most of the broadening is on the low wavelength side of λ_{LTM}. The bandwidth of chaotic output is primarily spreading towards the corresponding λ_{FP}. In contrast, the bandwidth associated with increasing entirely incoherent feedback ($D \geq 1/\mathrm{ns}$) spreads symmetrically about λ_{FP}. This prediction of the theoretical modeling can now be applied to the results of experimental studies and may ultimately become a method for indirectly determining the coherence state of the optical feedback. The shift in the wavelength with feedback factor η emerges as having potential for use interrogating the coherence of the feedback.

In conclusion, a new method for theoretically modeling the effective coherence of an optical feedback field has been developed and incorporated into a traveling wave model for dynamics in semiconductor lasers with delayed optical feedback. The method allows the coherence of the optical feedback field to be explored from fully coherent to fully incoherent. It remains to be confirmed, but the study to date suggests that much or some of the differences observed in detailed dynamics in experimental systems in different laboratories may be due to differences in the effective coherence of the optical feedback.

Acknowledgments

This work was partially supported by the Macquarie University Faculty of Science and Engineering Visiting Researcher Fellowship awarded to MR.

References

[1] D. Kane and K. Shore, eds., *Unlocking Dynamical Diversity: Optical Feedback Effects on Semiconductor Lasers* (Wiley & Sons, 2005).

[2] M. Sciamanna and K.A. Shore, "Physics and applications of laser diode chaos," *Nat. Photonics* **9**, 151 (2015).

[3] J. Ohtsubo, *Semiconductor Lasers: Stability, Instability and Chaos*, 4th ed. (Springer, 2017).

[4] A. Argyris, J. Bueno, and I. Fischer, "Photonic machine learning implementation for signal recovery in optical communications," *Sci. Reports* **8**, 8487 (2018).

[5] J. Bueno, D. Brunner, M. Soriano, and I. Fischer, "Conditions for reservoir computing performance using semiconductor lasers with delayed optical feedback," *Opt. Express* **25**, 2401 (2017).

[6] L. Keuninckx, M. Soriano, I. Fischer, C. Mirasso, R. Nguimdo, and G. Van der Sande, "Encryption key distribution via chaos synchronization," *Sci. Reports* **7**, 43428 (2017).

[7] R. Tkach and A. Chraplyvy, "Regimes of feedback effects in 1.5-μm distributed feedback lasers," *J. of Lightwave Technology* **4**, 1655 (1986).

[8] D. Lenstra, B. Verbeek, and A. Den Boef, "Coherence collapse in single-mode semiconductor lasers due to optical feedback," *IEEE J. of Quantum Electronics* **21**, 674 (1985).

[9] S. Donati and R.-H. Horng, "The diagram of feedback regimes revisited," *IEEE J. of Sel. Topics in Quantum Electron.* **19**, 1500309 (2013).

[10] M. Fleming and A. Mooradian, "Fundamental line broadening of single-mode (GaAl)As diode lasers," *Appl. Phys. Lett.* **38**, 511 (1981).

[11] J. Cohen, F. Wittgfrefe, M. Hoogerlan, and J. Woerdman, "Optical spectra of a semiconductor laser with incoherent optical feedback," *IEEE J. Quant. Electron.* **26**, 982 (1990).

[12] D. Kane and A. Willis, "External cavity diode lasers using different devices and collimating optics," *Appl. Opt.* **34**, 4316 (1995).

[13] D. Kane and V. Ta'eed, "Spatial beam profiles from a system of laser diode with optical feedback – the importance of interference," *Appl. Opt.* **40**, 4316 (2001).

[14] R. Ju, Y. Hong, and P. Spencer, "Semiconductor lasers subject to polarization-rotated optical feedback," in *SPIE Proc. Series* **6115**, p. 61150K (2006).

[15] C. Masoller, C. Serrat, and R. Vilaseca, "Modelling multi-longitudinal-mode semiconductor lasers with in coherent feedback," *Phys. Rev. A* **76**, 043814 (2007).

[16] M. Radziunas, "Traveling wave modeling of nonlinear dynamics in multisection semiconductor laser diodes," chap. 31 in *Handbook of Optoelectronic Device Modeling and Simulation: Lasers, Modulators, Photodetectors, Solar Cells, and Numerical Methods (vol. 2)*, J. Piprek ed., pp. 153–182 (CRC Press, 2017).

[17] J. Toomey and D. Kane, "Mapping the dynamic complexity of a semiconductor laser with optical feedback using permutation entropy," *Optics Express* **22**, 1713 (2014).

[18] M. Radziunas, V. Tronciu, C. Kürbis, H. Wenzel, and A. Wicht, “Study of microintegrated external-cavity diode lasers: simulations, analysis, and experiments,” *IEEE J. of Quantum Electronics* **51**, 2000408 (2015).

[19] M. Radziunas, *Opt. and Quant. Electron.* “Semiconductor ring laser with filtered optical feedback: traveling wave description and experimental validation,” **48**, 470 (2016).